Geophysical Research Letters, 24, 417-420, 1997

Sensing integrated water vapor along GPS ray paths

Randolph Ware, Chris Alber, Christian Rocken, Fredrick Solheim

University Corporation for Atmospheric Research, University Navstar Consortium, Boulder, Colorado

Abstract. We demonstrate sensing of integrated slant-path water vapor (SWV) along ray paths between Global Positioning System (GPS) satellites and receivers. We use double differencing to remove GPS receiver and satellite clock errors and 85-cm diameter choke ring antennas to reduce ground-reflected multipath. We compare more than 17,000 GPS and pointed radiometer double difference observations above 20^o elevation and find 1.3 mm rms agreement. Potential applications for SWV data include local and regional weather modeling and prediction, correction for slant wet delay effects in GPS surveying and orbit determination, and synthetic aperture radar (SAR) imaging. The method is viable during all weather conditions.

Introduction

The 24 Global Positioning System (GPS) satellites broadcast 1.2 and 1.6 GHz carrier signals based on atomic clocks. These signals can be tracked with high accuracy using commercial equipment sold at relatively low prices. An overview of GPS and its scientific applications is provided by *Herring* [1996].

Sensing Precipitable Water Vapor (PWV)

GPS sensing of precipitable water vapor with 1 mm (7%) accuracy was demonstrated by *Rocken et al.* [1993] using GPS methods developed for geodetic applications. The GPS geodetic method, described by *Dixon* [1991], can estimate time-varying atmospheric zenith path delay defined as:

$$\text{zenith path delay} = 10^{-6}\int_{\text{antenna}}^{\infty} N\,dz \qquad (1)$$

where dz has units of length in the zenith,

$$N = 77.6\frac{P}{T} + 3.73\times 10^5\frac{e}{T^2} \qquad (2)$$

is the refractivity of air, P is air pressure in mb, T is temperature in Kelvins and e is partial pressure of water vapor in mb.

If P is known, hydrostatic delay resulting from the first term in Equation (2) can be estimated and removed from the GPS solution. Zenith wet delay can then be estimated as a least squares fit that varies as the cosecant of the elevation angle, typically over intervals of 15 min to several hr. Zenith wet delay and PWV are related by:

$$\text{PWV} = \Pi \cdot \text{ zenith wet delay} \qquad (3)$$

where Π is a dimensionless conversion factor ~0.15 [*Hogg et al.,* 1981]. Surface temperature measurements can be used to estimate Π with an error less than 2% [*Bevis et al.,* 1992; 1994].

GPS sensed PWV is modeled using an average of all observed GPS rays, as shown in Fig. 1. This model is often inadequate. *Rocken et al.* [1991a] and *Davis et al.* [1993] found more than 20% azimuthal variation in radiometer measurements of integrated water vapor at 30^o elevation.

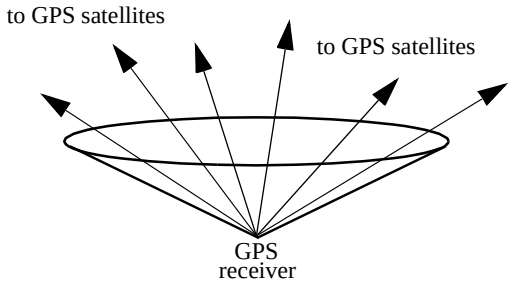

Figure 1. PWV is modeled as an average of all GPS satellite observations above the cut-off angle represented by the cone.

PWV data are potentially valuable for weather and climate modeling and prediction. *Kuo et al.* [1996] found significant improvement in precipitation forecasts when PWV data were assimilated in numerical weather prediction models. *Yuan et al.* [1993] simulated the use of PWV data in monitoring global and regional climate change and found up to 8 mm increase in tropical PWV resulting from a doubling of atmospheric CO_2.

Sensing Slant Water Vapor (SWV)

Integrated slant-path water vapor can be detected in GPS solution residuals, or directly by pointed radiometers. GPS signals are subject to:

$$\text{slant wet delay} = 10^{-6}\int_{\text{antenna}}^{\text{satellite}} N_{wet}\,ds \qquad (4)$$

where N_{wet} is the second term in Equation (2). Slant wet delay and ds have units of length along the ray path. Slant wet delay is related to SWV by:

$$\text{SWV} = \Pi \cdot \text{ slant wet delay} \qquad (5)$$

A slant path at 10^o elevation is shown in Fig. 2. At this angle the GPS ray traverses 6 km in height at ~34 km distance from the tracking site.

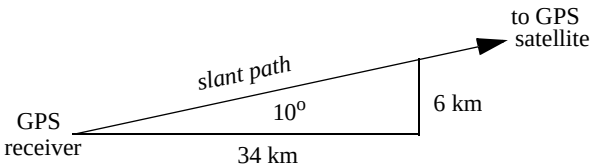

Figure 2. A slant ray path.

Refractive bending allows tracking of GPS satellites to the horizon and slightly lower [*Meehan et al.,* 1991; *Anderson,* 1994]. Taking earth's curvature and refractive bending into account, a GPS ray observed from the ground at 0^o elevation

through a standard atmosphere reaches 2 km in height at a distance of more than 200 km from the tracking site. GPS satellite tracks slightly below the horizon are shown in Fig 3.

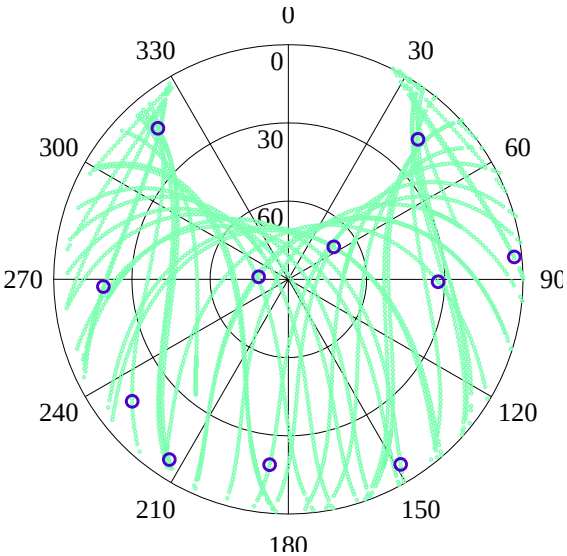

Figure 3. GPS satellite elevation and azimuth tracks (curves) observed from Table Mountain during 24 hours. Locations of satellites at a point in time are shown as open circles. Some of the eastern tracks reach as low as -0.7° elevation. To the west, mountains occlude tracking below 3°.

Experiment Description

We observed with GPS receivers and radiometers at Platteville and Table Mountain, Colorado, on May 21-23, 1996. The sites are relatively free from obstructions and are separated by 43 km. At each site we used Trimble SSI™ dual frequency receivers, Radiometrics WVR-1100™ radiometers, and 85-cm diameter choke ring antennas [*Solheim et al.*, 1996] to reduce ground-reflected multipath [*Alber*, 1996]. We observed with GPS at 30 sec intervals and with radiometers pointed toward each of the GPS satellites in view every ~8 min. A 20° elevation cutoff angle was chosen to exclude viewing of the horizon, buildings, or vegetation by the radiometer antenna sidelobes. Barometric data with 0.3 mb accuracy were recorded at each site. The radiometers viewed each GPS satellite for 1 sec at 23.8 GHz (5.5° beamwidth, full width half maximum) and 31.4 GHz (4.6° beamwidth) during an observation cycle. Beamwidth corrections are included in the radiometer software. Radiometer accuracy and calibration are described by *Solheim* [1993] and *Ware et al.* [1993].

Data Analysis

We analyzed GPS data using Bernese software [*Beutler et al.*, 1996], International GPS Service (IGS) precise orbits [*Neilan*, 1995], site coordinates fixed to the radiometer-corrected solution, and dry delays modeled from barometric data at each site. The software computes double differences defined as the difference in carrier phase of one satellite as observed from two sites, differenced again with a similar observation of a second satellite. Double differencing eliminates GPS transmitter and receiver clock errors and can be expressed as:

$$\text{double difference} = (\phi_{A1} - \phi_{B1}) - (\phi_{A2} - \phi_{B2}) \qquad (6)$$

where ϕ_{A1} is the carrier phase observation from site A of satellite 1, etc. We resolved all of the GPS carrier phase ambiguities (see for example *Beutler et al.*, 1996). The post-fit residuals of the GPS analysis include slant wet delays, unmodeled dry slant delays, multipath, orbit error and other unmodeled parameters along four ray paths.

Results and Discussion

Radiometer data, projected to the zenith, and their difference during the experiment are shown in Fig. 4. Scatter in each trace shows directional water vapor gradients and variation in the difference shows water vapor gradients between the two sites.

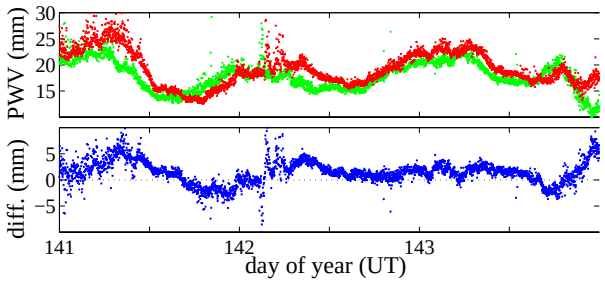

Figure 4. PWV derived from radiometer sensed SWV (upper) at Platteville and Table Mountain and their difference (lower). We attribute the spikes to moisture on the radiometer windows and to scattering of sunlight into the radiometers.

We used radiometer data for comparison with GPS data. SWV double differences sensed by radiometers and by GPS are compared in Fig. 5 and Table 1. The radiometer data were interpolated to match GPS observation times. Data degraded by moisture on the radiometer window were not included. The scatter in Fig. 5 maps roughly as the cosecant of the elevation angle.

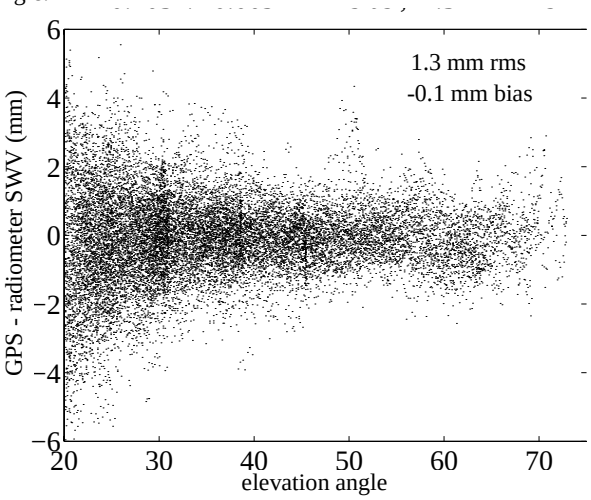

Figure 5. GPS minus radiometer sensed SWV double differences vs. elevation angle of the lowest satellite.

GPS signals are stabilized by atomic clocks, can be tracked in all weather conditions, and are affected by pressure field modeling error at low elevation angles. Radiometer data are affected by window moisture and reflected sunlight, are cali-

brated by tipping and by reference to a black body [*Solheim*, 1993], and are insensitive to pressure field modeling error.

We estimate the measurement accuracy of radiometer sensed SWV double differences using test data from pointed radiometers located 20 m apart. To approximate the radiometer data in Fig. 5 as closely as possible, we pointed the radiometers toward the GPS satellites in view, used a 20° elevation cut-off angle, excluded data degraded by moisture on the radiometer window, and interpolated to 30 sec intervals. The resulting 16,100 double differences demonstrate radiometer-pair sensitivity to SWV double differences of 0.7 mm rms. We can therefore estimate an upper limit on the GPS sensitivity to SWV double differences as the root square difference: $(1.3^2 - 0.7^2)^{1/2} = 1.1$ mm rms. This corresponds to a single ray path accuracy of 0.6 mm rms, assuming independent SWV along each of the four double difference ray paths. For the ~20 mm average PWV seen in Fig. 4, the single ray path SWV accuracy is 3% at zenith and 1% at 20° elevation.

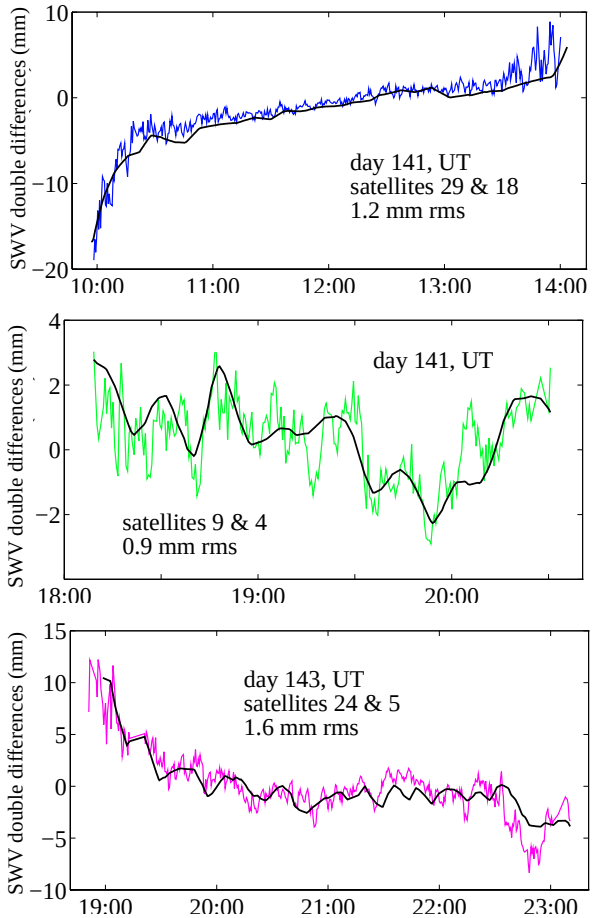

Figure 6. Examples of GPS (jagged) and radiometer (smooth) sensed SWV double differences and their agreement (rms). Note changes in scale.

GPS sensing of SWV along single ray paths with several mm precision should be possible using receiver clocks accurate to 10^{-12} sec to reduce errors from receiver clocks and from Selective Availability (S/A) dithering of GPS satellite clocks [*Rocken et al.*, 1991b].

Typical GPS and radiometer double differences and the corresponding satellite tracks are shown in Figs. 6 and 7. Similar SWV variations as large as 20 mm are seen in the GPS and radiometer data for periods greater than 30 min. For periods less than 30 min, variations as large as 7 mm are seen in the GPS data but not in the radiometer data. We attribute this to different sampling parameters for the two methods, and to multipath. The radiometers observed each satellite over a ~5° beamwidth at ~ 8 min intervals, whereas GPS sampled a volume surrounding the GPS rays [*Melbourne et al.*, 1994] less than 100 m in diameter at 30 sec intervals. We discuss a simulated SWV signal and multipath below.

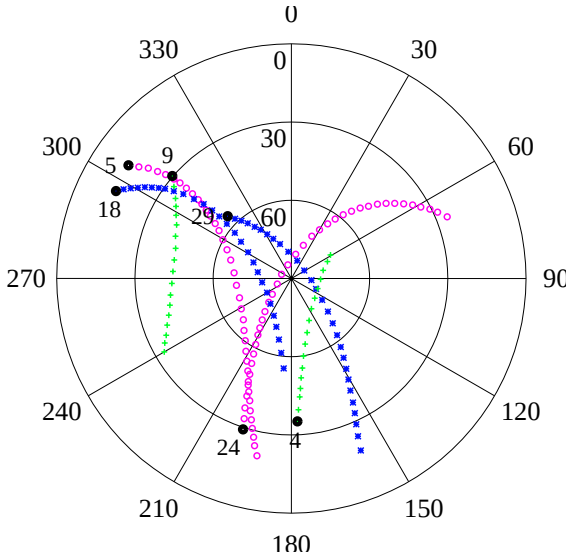

Figure 7. Directional tracks of the satellite pairs corresponding to Fig. 6, labeled by satellite number at the start of each track.

We simulate a typical SWV signal by ray tracing through a cell of water vapor (Fig. 8).

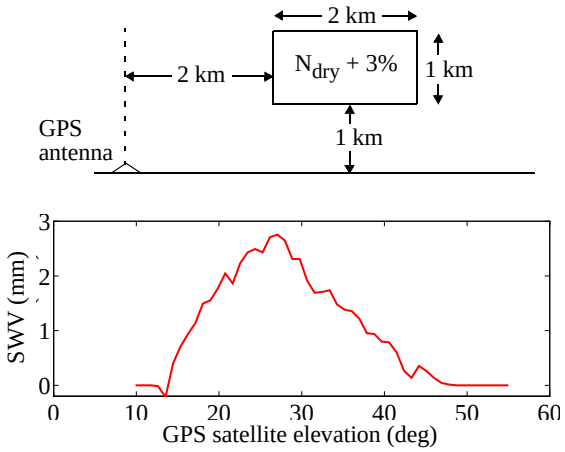

Figure 8. Ray tracing through a two dimensional curved atmosphere including a 3% refractivity variation (upper panel) generates a ~3 mm SWV signal (lower panel).

The water vapor cell produces ~3 mm of SWV signal near 30°. We see similar short period variations in the real (Fig. 6) and simulated (Fig. 8) GPS data. Even larger signals would be

generated by 10% refractivity variations that occur in clear air [*Konrad*, 1970] and in clouds [*Campen et al.*, 1961].

Other sources of short period variations in the GPS data include receiver system noise and multipath. Receiver noise is typically ~1 mm. Separate tests determined that multipath effects were 1.6 mm rms for the 85-cm choke ring antennas, including several mm variations near 20^o elevation that repeat in sidereal time [*Alber*, 1996]. The ~3 mm GPS variations seen in the center panel of Fig. 6 occur at elevation angles larger than 30^o and are not likely to be caused by multipath. At elevation angles near 20^o where ground-reflected multipath is expected, variations in the GPS double differences do not repeat in sidereal time and are therefore probably not dominated by multipath. Thus, we attribute most of the short period variation observed in the GPS data to SWV signal.

Table 1. GPS vs. radiometer sensed SWV (20^o cutoff).

day of year	number of double difference observations	GPS - radiometer sensed SWV double differences (mm rms)
141	4,167	1.1
142	6,364	1.3
143	7,369	1.3
all	**17,900**	**1.3**

GPS sensing of SWV should be possible down to 0^o elevation and slightly below. At low elevation angles the method could be used to detect water vapor associated with fronts, storms, and other weather and climate phenomena at distances of several hundred km. Either single path or double difference SWV data can potentially be assimilated in numerical weather models. SWV data could be observed using continuous GPS tracking networks [*Businger et al.*, 1996], could be used to complement GPS occultation measurements [*Ware et al.*, 1996], and to correct for wet delay effects in GPS surveying, orbit determination and synthetic aperture radar (SAR) imaging of crustal deformation and topography [*Meade and Sandwell*, 1996].

Conclusions

We have demonstrated that GPS and pointed radiometer double difference SWV observations agree to 1.3 mm rms above 20^o elevation if care is taken to reduce multipath and if site coordinates and satellite orbits are well known. Further work is needed to develop GPS sensing of SWV along single ray paths, to develop methods for assimilation of SWV data into numerical weather prediction models, and to validate the method below 20^o elevation.

Acknowledgments. NSF grant EAR-9406153 sponsored the work. Equipment was loaned by the UNAVCO Facility (EAR-9116461) and Radiometrics, Inc.

References

Alber, C., Millimeter Precision GPS Surveying and GPS Sensing of Slant Path Water Vapor, Ph.D. Thesis, Univ. Colorado, Dec. 1996.

Anderson, K., Tropospheric Refractivity Profiles Inferred from Low-Elevation Angle Measurements of Global Positioning System Signals, *AGARD-CP-576-2*, 1994.

Beutler, G., E. Brockman, S. Fankhauser, W. Gurtner, J. Johnson, L. Mervart, M. Rothacher, S. Schaer, T. Springer, and R. Weber, Bernese GPS Software Version 4.0, Univ. Berne, September, 1996.

Bevis, M., S. Businger, T. Herring, C. Rocken, R. Anthes, and R. Ware, GPS Meteorology: Remote Sensing of Atmospheric Water Vapor using the Global Positioning System, *J. Geophys. Res., 97*, 15,787-15,801, 1992.

Bevis, M., S. Businger, S. Chiswell, T. Herring, R. Anthes, C. Rocken, and R. Ware, GPS Meteorology: Mapping Zenith Wet Delays onto Precipitable Water, *J. Appl. Meteorol., 33*, 379-386, 1994.

Businger, S., S. Chiswell, M. Bevis, J. Duan, R. Anthes, C. Rocken, R. Ware, T. Van Hove, and F. Solheim, The Promise of GPS in Atmospheric Monitoring, *Bull. Am. Meteorol. Soc., 77*, 5-18, 1996.

Campen, C., R. Cunningham, and V. Plank, Electromagnetic wave propagation in the lower atmosphere, *Handbook of Geophysics*, New York, Macmillan, ch. 13, 5-11, 1961.

Davis, J., G. Elgered, A. Niell, and C. Kuehn, Ground-based measurement of gradients in the "wet" radio refractivity of air, *Rad. Sci., 28*, 1003-1018, 1993.

Dixon, T., An Introduction to the Global Positioning System and some geological applications, *Rev. Geophys., 29*, 249-276, 1991.

Hogg, D., F. Guiraud, and M. Decker, Measurement of Excess Radio Transmission Length on Earth-Space Paths, *Astron. Astrophys., 95*, 304-307, 1981.

Herring, T., The Global Positioning System, *Sci. Am.*, 44-50, Feb., 1996.

Konrad, T., The dynamics of convective process in clear air as seen by radar, *J. Atmos. Sci., 27*, 1138, 1970.

Kuo, Y.-H., X. Zou, and Y.-R. Guo, Variational Assimilation of Precipitable Water Using a Nonhydostatic Mesoscale Adjoint Model, *Mon. Weather Rev., 124*, 122-147, 1996.

Meade, C. and D. Sandwell, Synthetic Aperture Radar for Geodesy, *Science, 273*, 1181-1182, 1996.

Meehan, T., E. Kursinski, G. Hajj, J. Srinivasan, and S. DiNardo, Analysis of Global Positioning System Signals Occulted by the Atmosphere as Tracked From Mauna Kea, *Eos Trans. AGU, 72*, 372, 1991.

Melbourne, W., E. Davis, C. Duncan, G. Hajj, K. Hardy, E. Kursinski, T. Meehan, L. Young, and T. Yunck, The Application of Spaceborne GPS to Atmospheric Limb Sounding and Global Change Monitoring, *JPL Pub. 94-18*, 1994.

Neilan, R., The Evolution of the IGS Global Network, Current Status and Future Prospects, International GPS Service for Geodynamics, 1994 Annual Report, *JPL Pub. 95-18*, 25-34, 1995.

Rocken, C., J. Johnson, R. Neilan, M. Cerezo, J. Jordan, M. Falls, L. Nelson, R. Ware, and M. Hayes, The Measurement of Atmospheric Water Vapor: Radiometer Comparison and Spatial Variations, *IEEE Trans. Geosci. & Remote Sensing, 29*, 3 - 8, 1991a.

Rocken, C., and C. Meertens, Monitoring selective availability dither frequencies and their effect on GPS data, *Bull. Geodesique*, 162-169, 1991b.

Rocken, C., R. Ware, T. Van Hove, F. Solheim, C. Alber, and J. Johnson, Sensing Atmospheric Water Vapor with the Global Positioning System, *Geophys. Res. Lett., 20*, 2631-2634, 1993.

Solheim, F., C. Alber, R. Ware, and C. Rocken, Pointed Radiometry for Coordinate and Orbit Accuracy, *Augmenting GPS Infrastructure for Geoscience Applications*, Nat. Acad. Press (in press), 1996.

Solheim, F., Use of Pointed Water Vapor Radiometers to Improve GPS Surveying Accuracy, Ph.D. Thesis, Univ. Colorado, Dec. 1993.

Ware, R., C. Rocken, F. Solheim, T. Van Hove, C. Alber, and J. Johnson, Pointed Water Vapor Radiometer Corrections for Accurate GPS Surveying, *Geophys. Res. Lett., 20*, 2635-2638, 1993.

Ware, R., M. Exner, D. Feng, M. Gorbunov, K. Hardy, B. Herman, H. K. Kuo, T. Meehan, W. Melbourne, C. Rocken, W. Schreiner, S. Sokolovskiy, F. Solheim, X. Zou, R. Anthes, S. Businger, and K. Trenberth, GPS Sounding the Atmosphere from Low Earth Orbit, Preliminary Results, *Bull. Am. Meteorol. Soc., 77*, 5-18, 1996.

Yuan, L., R. Anthes, R. Ware, C. Rocken, W. Bonner, M. Bevis, and S. Businger, Sensing Climate Change Using the Global Positioning System, *J. Geophys. Res., 98*, 14,925-14,937, 1993.

R. Ware, C. Alber, C. Rocken, and F. Solheim, University Corporation for Atmospheric Research, Boulder, CO, 80307. (e-mail: ware@ucar.edu)

(Received October 8, 1996; accepted November 15, 1996)